GEOPHYSICS. VOL. 54, NO. 9 (SEPTEMBER 1989); P. 1180–1192, 10 FIGS.

A new approach to modeling the electromagnetic response of conductive media

K. H. Lee*, G. Liu‡, and H. F. Morrison‡

ABSTRACT

We introduce a new and potentially useful method for computing electromagnetic (EM) responses of arbitrary conductivity distributions in the earth. The diffusive EM field is known to have a unique integral representation in terms of a fictitious wave field that satisfies a wave equation. We show that this integral transform can be extended to include vector fields. Our algorithm takes advantage of this relationship between the wave field and the actual EM field. Specifically, numerical computation is carried out for the wave field, and the result is transformed back to the EM field in the time domain.

The proposed approach has been successfully demonstrated using two-dimensional (2-D) models. The appropriate TE-mode diffusion equation in the time domain for the electric field is initially transformed into a scalar wave equation in an imaginary q domain, where q is a time-like variable. The corresponding scalar wave field is computed numerically using an explicit q-stepping technique. Standard finite-difference methods are used to approximate the fields, and absorbing boundary conditions are implemented. The computed wave field is then transformed back to the time domain. The result agrees fairly well with the solution computed directly in the time domain.

We also present an approach for general three-dimensional (3-D) EM problems for future studies. In this approach, Maxwell's equations in the time domain are first transformed into a system of coupled first-order wave equations in the q domain. These coupled equations are slightly modified and then cast into a "symmetric" and "divergence-free" form. We show that it is to this particular form of equations that numerical schemes developed for solving wave equations can be applied efficiently.

INTRODUCTION

Electromagnetic (EM) methods in geophysics have been used for many years to determine the electrical conductivity of the subsurface. The major application in Western countries has been in the search for mineral deposits, with lesser applications in groundwater, petroleum exploration, and crustal studies. In the Soviet Union, EM methods have played a major role both in petroleum exploration and in mineral exploration. In all these applications, the depth of interest requires low frequencies, usually less than 30 kHz; and for typical earth conductivities, the conduction current is orders of magnitude greater than the displacement currents. The resulting second-order partial differential equation describing the behavior of the fields is, in fact, a diffusion equation for which the solutions are quite different from those of the more familar wave equation encountered in seismic wave propagation or radar. Concepts of pulse or wavelet propagation or of pulse traveltime and the construction of reflectivity images of subsurface structure are not possible for solutions that do not allow well defined group velocity. The difficulty of depicting the solutions for the diffusion equation in all but simple, elementary situations is one practical reason for the slow acceptance of EM conductivity mapping in new applications.

There are also numerical and computational complications in using EM methods. Whereas perfectly useful model realizations can be obtained with simple ray-tracing algorithms in seismic studies, the EM responses for the same models require a complete solution to a formal boundary

Manuscript received by the Editor October 11, 1988; revised manuscript received March 6, 1989.
*Lawrence Berkeley Laboratory, Bldg. 50 E, University of California, 1 Cyclotron Road, Berkeley, CA 94720.
‡Department of Materials Science and Mineral Engineering, 414 Hearst Mining Bldg., University of California, Berkeley, CA 94720.

value problem—usually a time-consuming process, since the solution is obtained from the vector diffusion equation.

There have been great strides in obtaining efficient solutions for certain classes of EM problems. The methods break down basically into differential and integral equation techniques.

Differential equation solutions were used as early as 1975 by Lines and Jones for magnetotelluric (MT) problems, and the technique has grown in power and efficiency ever since (Reddy et al., 1977; Pridmore, 1978). These solutions are usually obtained in the frequency domain at discrete frequencies. Although the methods can be used to model arbitrary conductivity structures, practical applications have been limited because the number of equations involved is too great for available computers.

Lee et al. (1981) and Best et al. (1985) presented interesting numerical solutions based on a scheme called the hybrid method (Scheen, 1978). Later, Gupta et al. (1987) reported a much improved numerical solution based on the compact finite-element technique, a condensed version of the hybrid method. The method basically consists of the finite-element technique, but the computational domain is confined to the inhomogeneous region on whose boundary Green's functions are used to enforce boundary conditions.

Numerical solutions using the integral equation technique have been presented by Raiche (1974), Weidelt (1975), Hohmann (1975), and Meyer (1977). In this method the number of equations is reduced to essentially the number of inhomogeneous elements, but the resulting matrix is full and generally asymmetric. Further, each element of the matrix is derived from a combination of Green's functions whose computation is difficult; this step often dominates the consumption of computer time.

Integral equation solutions, in either the time or the frequency domain, also have problems associated with the representation of the scattering currents, especially if the host conductivity is low. Newman and Hohmann (1988) provide an elegant analysis of this problem and show the importance of carefully constructing a divergence-free and curl-free representation of the scattering current. Their solution involves a linear combination of closed current tubes concentric with the center of rectangular prisms as the divergence-free basis functions and constant current or pulse basis functions for the curl-free component. The solution is in the frequency domain and the time-domain response is obtained by inverse Fourier transformation. This combination works very well for cube-like bodies and provides the best, fastest algorithm yet produced for handling arbitrary conductivity contrasts.

3-D direct time-stepping solutions for the EM diffusion equations have been obtained by San Filipo and Hohmann (1985) with an integral equation formulation, again using tubes to represent the divergence-free terms in the solution. 2-D time-domain solutions have been presented by Oristaglio and Hohmann (1984) and Adhidjaja et al. (1985) using an explicit time-stepping technique for a finite-difference approach. Kuo and Cho (1980) and Goldman et al. (1986) also developed 2-D time-domain solutions using the finite-element method with explicit and implicit time-stepping schemes, respectively.

Several studies have implied interesting parallelism between the mathematical form for the EM diffusion equation in layered media and the seismic wave equation in the same media (Weidelt, 1972; Kunetz, 1972; and Levy et al., 1988). These studies led us to investigate a more fundamental relationship between the diffusion and wave equations, to try to find out if, in fact, the diffusion equation for a field $\mathbf{E}$ in time t might not be transferable to a wave equation for a field $\mathbf{U}$ in a time-like variable q. This field $\mathbf{U}$ would be dispersionless and would have a well defined phase, as well as a group, velocity. For any given conductivity distribution, $\mathbf{U}$ could be obtained by any of the time-stepping methods available for wave-equation modeling. The solution could presumably be obtained for a pulse or a wavelet and the results portrayed just as seismic or radar results are shown. The solution in q would then be transformed back to time to obtain the field actually measured. A further and equally intriguing possibility is that the inverse transform could be used to transform field data in time to the wave field in q for analysis using migration or even more sophisticated wave-equation imaging or tomographic techniques.

In this paper such a transform is presented, and the concept is tested numerically using 2-D models. We first show a relationship between the diffusive EM field in the time domain and its corresponding wave field in the q domain. The transform process presented here is similar to the one given by Lavrent'ev et al. (1980), but has been generalized to include vector EM fields. The modeling approach consists of two steps: first, the numerical computation of the wave field is carried out in the q domain, and then the resulting wave field is transformed back to the EM field in the time domain.

THEORY

In this section we describe the formal relationship between the diffusive EM field in the time domain and the associated wave field in the q domain.

The EM fields are governed by Maxwell's equations. In the presence of a current source $\mathbf{J}^s$ they are

$$\nabla \times \mathbf{E}(\mathbf{r}, t) = -\frac{\partial}{\partial t}\mathbf{B}(\mathbf{r}, t), \tag{1}$$

$$\nabla \times \mathbf{H}(\mathbf{r}, t) = \frac{\partial}{\partial t}\mathbf{D}(\mathbf{r}, t) + \mathbf{J}^c(\mathbf{r}, t) + \mathbf{J}^s(\mathbf{r}, t). \tag{2}$$

Here the conduction current $\mathbf{J}^c$ is related to the electric field by Ohm's law

$$\mathbf{J}^c(\mathbf{r}, t) = \sigma(\mathbf{r})\mathbf{E}(\mathbf{r}, t).$$

When we substitute the constitutive relations

$$\mathbf{B}(\mathbf{r}, t) = \mu\mathbf{H}(\mathbf{r}, t)$$

and

$$\mathbf{D}(\mathbf{r}, t) = \varepsilon(\mathbf{r})\mathbf{E}(\mathbf{r}, t)$$

into equations (1) and (2), the electric field satisfies

$$\nabla \times \nabla \times \mathbf{E}(\mathbf{r}, t) + \mu\sigma(\mathbf{r})\frac{\partial}{\partial t}\mathbf{E}(\mathbf{r}, t) + \mu\varepsilon(\mathbf{r})\frac{\partial^2}{\partial t^2}\mathbf{E}(\mathbf{r}, t) = \mathbf{S}(\mathbf{r}, t), \tag{3}$$

where μ is assumed constant and equal to the value in free space and the source term $\mathbf{S}(\mathbf{r}, t)$, identified as

$$\mathbf{S}(\mathbf{r}, t) = -\mu \frac{\partial}{\partial t} \mathbf{J}^s(\mathbf{r}, t),$$

is assumed to be causal. Throughout the derivation the medium is considered linear and isotropic. If we further assume that the displacement current is negligible, equation (3) simplifies to

$$\nabla \times \nabla \times \mathbf{E}(\mathbf{r}, t) + \mu\sigma(\mathbf{r}) \frac{\partial}{\partial t} \mathbf{E}(\mathbf{r}, t) = \mathbf{S}(\mathbf{r}, t). \tag{4}$$

The corresponding initial and boundary conditions are written formally as

$$\mathbf{E}(\mathbf{r}, 0) = \mathbf{0}, \qquad \mathbf{E}_\Gamma = \mathbf{E}(\mathbf{r}_b, t); \qquad t > 0,$$

where Γ is the boundary of the volume V at $\mathbf{r} = \mathbf{r}_b$. We now introduce functions $\mathbf{U}(\mathbf{r}, q)$ and $\mathbf{F}(\mathbf{r}, q)$ such that

$$\nabla \times \nabla \times \mathbf{U}(\mathbf{r}, q) + \mu\sigma(\mathbf{r}) \frac{\partial^2}{\partial q^2} \mathbf{U}(\mathbf{r}, q) = \mathbf{F}(\mathbf{r}, q),$$

$$\mathbf{U}(\mathbf{r}, 0) = \frac{\partial}{\partial q} \mathbf{U}(\mathbf{r}, q)\Big|_{q=0} = 0,$$

and

$$\mathbf{U}|_\Gamma = \mathbf{U}(\mathbf{r}_b, q); \qquad q > 0. \tag{5}$$

After we make the connection between equations (4) and (5), it is clear that the independent variable q has the dimension of square root of time. The function $\mathbf{U}(\mathbf{r}, q)$ would behave as if it were a propagating wave with a velocity of $(\mu\sigma)^{-1/2}$ in $\mathrm{m}/\sqrt{\mathrm{s}}$.

A unique relation between $\mathbf{E}(\mathbf{r}, t)$ of the vector diffusion equation (4) and $\mathbf{U}(\mathbf{r}, q)$ of the vector wave equation (5) is now derived. Laplace transforming equations (4) and (5) from t to s and from q to p, respectively, we find

$$\begin{aligned} &\nabla \times \nabla \times \hat{\mathbf{E}}(\mathbf{r}, s) + \mu\sigma(\mathbf{r}) s \hat{\mathbf{E}}(\mathbf{r}, s) = \hat{\mathbf{S}}(\mathbf{r}, s), \\ &\hat{\mathbf{E}}\Big|_\Gamma = \hat{\mathbf{E}}(\mathbf{r}_b, s); \qquad -\frac{\pi}{2} < \arg(s) < +\frac{\pi}{2}, \end{aligned} \tag{6}$$

and

$$\nabla \times \nabla \times \hat{\mathbf{U}}(\mathbf{r}, p) + \mu\sigma(\mathbf{r}) p^2 \hat{\mathbf{U}}(\mathbf{r}, p) = \hat{\mathbf{F}}(\mathbf{r}, p),$$

$$\hat{\mathbf{U}}\Big|_\Gamma = \hat{\mathbf{U}}(\mathbf{r}_b, p); \qquad -\frac{\pi}{2} < \arg(p) < +\frac{\pi}{2}. \tag{7}$$

If we let $s = p^2$, equation (6) becomes

$$\nabla \times \nabla \times \hat{\mathbf{E}}(\mathbf{r}, p^2) + \mu\sigma(\mathbf{r}) p^2 \hat{\mathbf{E}}(\mathbf{r}, p^2) = \hat{\mathbf{S}}(\mathbf{r}, p^2),$$

$$\hat{\mathbf{E}}\Big|_\Gamma = \hat{\mathbf{E}}(\mathbf{r}_b, p^2); \qquad -\frac{\pi}{4} < \arg(p) < +\frac{\pi}{4}. \tag{8}$$

When we subtract the differential equation in equations (8) from that in equations (7), with additional conditions

$$\hat{\mathbf{S}}(\mathbf{r}, p^2) = \hat{\mathbf{F}}(\mathbf{r}, p)$$

and

$$\hat{\mathbf{E}}(\mathbf{r}_b, p^2) = \hat{\mathbf{U}}(\mathbf{r}_b, p), \tag{9}$$

we find that

$$\nabla \times \nabla \times \hat{\mathbf{D}}(\mathbf{r}, p) + \mu\sigma(\mathbf{r}) p^2 \hat{\mathbf{D}}(\mathbf{r}, p) = 0$$

and

$$\hat{\mathbf{D}}|_\Gamma = 0; \qquad -\frac{\pi}{4} < \arg(p) < +\frac{\pi}{4}, \tag{10}$$

where $\hat{\mathbf{D}}(\mathbf{r}, p)$ is defined as the difference between $\hat{\mathbf{E}}(\mathbf{r}_b, p^2)$ and $\hat{\mathbf{U}}(\mathbf{r}, p)$. Multiplying both sides of the first equation in equations (10) by $\hat{\mathbf{D}}^*(\mathbf{r}, p)$, integrating over the volume V bounded by the surface Γ, and applying a vector identity and the divergence theorem, we obtain

$$\int_V |\nabla \times \hat{\mathbf{D}}(\mathbf{r}, p)|^2 \, dv + \mu p^2 \int_V \sigma(\mathbf{r}) |\hat{\mathbf{D}}(\mathbf{r}, p)|^2 \, dv = 0;$$

$$-\frac{\pi}{4} < \arg(p) < +\frac{\pi}{4},$$

which can be true only if

$$\hat{\mathbf{E}}(\mathbf{r}, p^2) = \hat{\mathbf{U}}(\mathbf{r}, p).$$

This result implies, after dropping the spatial variable $\mathbf{r}$, that

$$\int_0^\infty \mathbf{E}(t) e^{-p^2 t} \, dt = \int_0^\infty \mathbf{U}(q) e^{-pq} \, dq,$$

or, from $s = p^2$ with $-\pi/2 < \arg(s) < +\pi/2$,

$$\int_0^\infty \mathbf{E}(t) e^{-st} \, dt = \int_0^\infty \mathbf{U}(q) e^{-\sqrt{s}q} \, dq.$$

Inverse Laplace transforming (from s to t) both sides of the last equation, we finally obtain the integral relation between the electric field $\mathbf{E}(t)$ and the wave field $\mathbf{U}(q)$:

$$\mathbf{E}(t) = \frac{1}{2\sqrt{\pi t^3}} \int_0^\infty q e^{-q^2/4t} \mathbf{U}(q) \, dq. \tag{11}$$

The necessary conditions (9) also result in the identical relation for the source and boundary values in the q and t domains. This transformation involves only t and q and is independent of $\mathbf{r}$.

An interesting aspect of the transformation can be seen through the following spectral analysis. Fourier transforming differential equations (4) and (5) from t to ω and q to ν, respectively, we have

$$\nabla \times \nabla \times + i\omega\mu\sigma \tilde{\mathbf{E}}(\omega) = \mathbf{0}, \tag{12a}$$

assuming an $e^{+i\omega t}$ time dependence, and

$$\nabla \times \nabla \times \tilde{\mathbf{U}}(\nu) - \nu^2 \mu\sigma \tilde{\mathbf{U}}(\nu) = \mathbf{0}. \tag{12b}$$

We have dropped the source terms from these equations for the sake of simplicity. Notice that equation (12b) could also result if a change of variable, $\omega = i\nu^2$, is made to equation (12a). This amounts to an analytic continuation of electric fields on the real ω axis to fields on a contour $\nu = \sqrt{-i\omega}$ with $\Phi(\nu) = \pm\pi/4$ in the complex ω plane. In this connection, the function $B(x)$ in the MT inverse study by Weidelt (1972) is similar in nature to the wave field $\mathbf{U}(q)$. This similarity can

also be observed between the discrete form of $\tilde{U}(\nu)$ and the "pseudo-impulse series" q_m derived from the modified impedance in the MT imaging studies by Kunetz (1972) and later by Levy et al. (1988).

For further analysis, an important application of this transformation is the construction of wave fields from the time-domain data $\mathbf{E}(t)$. This process is essentially an inverse problem for the wave field $\mathbf{U}(q)$. As was pointed out by Weidelt (1972), the problem is ill-posed because the kernel of the integral is exponentially damped. Nevertheless, if successfully implemented, it could be used to develop an EM imaging technique, a process which has not been possible in the past due to the diffusive nature of the field. Studies related to this subject from the point of view of inverse scattering have been presented earlier by Isaev and Filatov (1981) and Filatov (1984). A preliminary result in reconstructing the wave field has been reported by Lee (1987).

Our primary objective in this study, however, is to apply the transformation technique to the numerical modeling of EM fields. In this application, we first obtain the wave field $\mathbf{U}(q)$ numerically for a corresponding source $\mathbf{F}(q)$. The next step is straightforward using the integral given by equation (11). This numerical modeling scheme is particularly attractive not only because many efficient wave equation algorithms are readily available, but because it is easy to implement these algorithms on modern computers, especially on those with parallel processing capabilities.

2-D NUMERICAL SCHEMES

One of the main objectives of this paper is to demonstrate a new numerical method that is accurate and potentially faster than conventional methods. To begin, we consider a 2-D EM problem. The model consists of a 2-D earth with a line source of current polarized in the direction parallel to the strike. A Cartesian coordinate system is employed with its y-axis parallel to the strike and the positive z-axis pointing downward.

In 2-D the problem is scalar. The electric field E_y satisfies the second-order diffusion equation

$$\nabla^2 E - \mu\sigma \frac{\partial}{\partial t} E = -S \tag{13}$$

in the time domain. Numerical solutions to this equation have been given by Kuo and Cho (1980), Oristaglio and Hohmann (1984), and Goldman et al. (1986). Equation (13) can be formally transformed to

$$\nabla^2 U - \mu\sigma \frac{\partial^2}{\partial q^2} U = -F \tag{14}$$

in the q domain. The subscript y is omitted from these equations for simplicity and ∇^2 now indicates the 2-D Laplacian in x and z. All model results presented in this paper are numerical solutions based on the scalar wave equation (14).

A simple analytic example that illustrates the concept of field transformation is given below. By switching off at $t = 0^+$ a steady unit current through a line source at the origin ($x = z = 0$), the time-domain source is

$$S = \mu\delta(x)\,\delta(z)\,\delta(t - 0^+).$$

To find the corresponding q-domain source F, we first write, from equation (11),

$$\mu\delta(x)\,\delta(z)\,\delta(t - 0^+) = \frac{1}{2\sqrt{\pi t^3}} \int_0^\infty q e^{-q^2/4t} F\, dq$$

and take the Laplace transform (t to s) of both sides of the equation. Then,

$$\mu\delta(x)\,\delta(z) = \int_0^\infty e^{-\sqrt{s}q} F\, dq;$$

this is possible only if

$$F = \mu\delta(x)\,\delta(z)\,\delta(q - 0^+).$$

In a homogeneous whole space, solutions to equations (13) and (14) in the presence of sources S and F are

$$E = \frac{\mu}{4\pi} \frac{e^{-\mu\sigma\rho^2/4t}}{t},$$

and

$$U = \frac{\mu}{2\pi} \frac{H(q - \sqrt{\mu\sigma}\rho)}{\sqrt{q^2 - \mu\sigma\rho^2}},$$

respectively. Here $\rho^2 = x^2 + z^2$, and $H(\cdot)$ is a unit step function. Substituting the wave field U into the integral (11) results in the electric field E given above.

Another analytic example of the transform method is demonstrated using a circular cylinder in a whole space of conductivity 0.0033 S/m (Figure 1). The source waveform used in the q domain is the first derivative of a Gaussian pulse

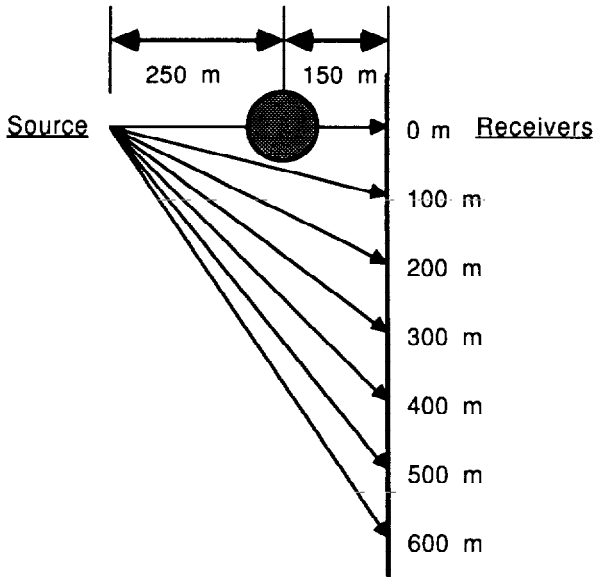

Fig. 1. A 0.1 S/m circular cylinder of radius 50 m in a uniform 0.0033 S/m whole space. A line source is located at 250 m to the left of the center of the cylinder, and the electric field is computed at positions on the vertical line 150 m to the right of the center of the cylinder.

$$F(q) = -\frac{(q - q_0)}{\alpha^2} e^{-(q-q_0)^2/2\alpha^2},$$

whose time-domain equivalent can be obtained by using equation (11). Constants used for this exercise are $\alpha = 0.001\sqrt{s}$ and $q_0 = 0.04\sqrt{s}$. The total-field solution for the wave equation (14) is shown in Figure 2. As is expected, the wave field computed in the shadow zone (zero offset) shows a slight delay in arrival time with a substantial decrease in amplitude. Traces of multiple reflections are also present. These wave fields are then transformed back to the time domain and the results (dashed lines) are compared with the other independently obtained time-domain solutions (solid lines) in Figure 3. With minor differences, due to the truncated summation of the Bessel functions that represent the analytic solutions in the frequency domain (Harrington, 1961), these two solutions are in good agreement.

NUMERICAL SOLUTIONS

We have used a standard finite-difference method with an explicit q-stepping scheme to solve the scalar wave equation (14) and have simulated the numerical domain by a grid whose top boundary is fixed at the air-earth interface. At this interface, a modified version of the integral boundary condition (Oristaglio and Hohmann, 1984) has been implemented (see Appendix B).

In order to advance the electric fields to the next q step, the explicit scheme requires field values at the current step and one step before at every node. The increment in q is strictly dictated by the Courant-Friedrichs-Lewy (CFL) stability condition for hyperbolic equations (Mitchell and Griffiths, 1980). For a 2-D scheme, the q increment is given by

$$\Delta q < \frac{h_{\min}}{\sqrt{2}v_{\max}}, \tag{15}$$

where v is the phase velocity defined by $(\mu\sigma)^{-1/2}$ and h is the grid spacing. From numerical considerations, Δq and h are inherently related to the source waveform for a given conductivity model. The waveform we have used for this application is the Gaussian pulse

$$F(q) = e^{-(q-q_0)^2/2\alpha^2}.$$

The parameters q_0 and α should be chosen such that the source field becomes negligible at $q = 0$; therefore, the source field can be considered effectively causal. In determining the grid spacing h, we first examine the frequency spectrum of the Gaussian pulse. With $q_0 = 0$ for convenience, we have

$$\tilde{F}(\nu) = \int_{-\infty}^{+\infty} F(q) e^{-i2\pi\nu q}\, dq = \sqrt{2\pi}\alpha e^{-2\pi^2\nu^2\alpha^2}.$$

The source energy contained within a cutoff frequency β may be found as

$$\int_{-\beta}^{+\beta} |\tilde{F}(\nu)|^2\, d\nu = \sqrt{\pi}\alpha \operatorname{erf}(2\pi\alpha\beta),$$

from which we find that about 85 percent of the source energy would be accounted for if we choose $\beta = (2\pi\alpha)^{-1}$. Another independent factor that should be considered in determining the grid spacing is the number of samples per wavelength λ. For the type of difference operator we used, second order both in space and q, 10 to 14 samples per wavelength is adequate. Using this information, we can now estimate the grid spacing as

$$h_{\min} < \frac{\lambda_{\min}}{10} = \frac{1}{10}\frac{v_{\min}}{\beta} = \frac{\pi\alpha v_{\min}}{5}, \tag{16}$$

from which we finally estimate the maximum Δq as

$$\Delta q_{\max} = \frac{\pi\alpha}{5\sqrt{2}}\frac{v_{\min}}{v_{\max}} = 0.44\alpha\frac{v_{\min}}{v_{\max}}. \tag{17}$$

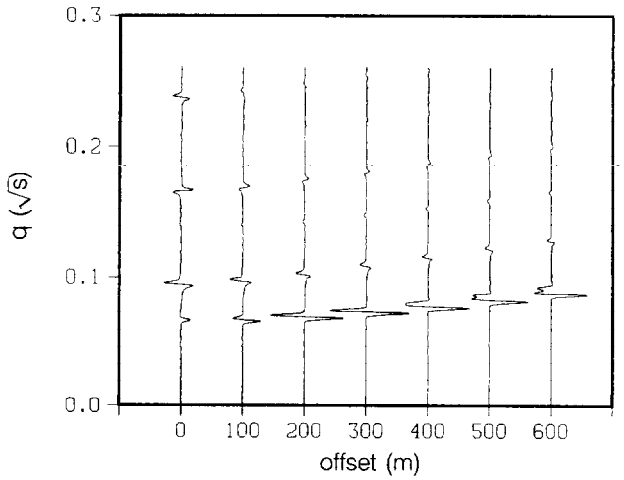

Fig. 2. q-domain responses at offsets of 0, 100, 200, 300, 400, 500, and 600 m.

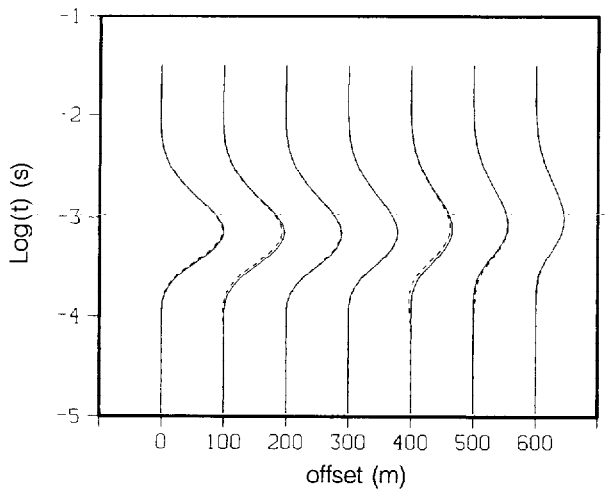

FIG. 3. A comparison between the direct time-domain solution and the transformed solution at offsets of 0, 100, 200, 300, 400, 500, and 600 m. Solid lines represent the direct solution and dashed lines are the transformed solution.

The wave-field velocity is proportional to the square root of the resistivity. The ratio of the minimum velocity to the maximum velocity, i.e., the resistivity contrast, in a heterogeneous medium is, therefore, equal to the square root of the ratio of the minimum resistivity to the maximum resistivity. This means that the step size in q given by equation (17) would decrease with increasing resistivity contrast. This result implies that modeling in the q domain becomes less efficient when the resistivity contrast is very large.

We now present two numerical examples to demonstrate and verify the q-domain approach for EM modeling. The first case concerns the numerical computation of the electric field in the q domain and subsequent verification of this result with the analytic solution. The model is a homogeneous half-space of 0.01 S/m conductivity; two line sources are used to excite the medium. Currents in these two lines are made to flow in opposite directions with the positive source located at the origin and the negative one at $x = -300$ m. In this example, parameters used to define the Gaussian pulse are $q_0 = 0.06\sqrt{s}$ and $\alpha = 0.01\sqrt{s}$. To check our finite-difference code, we used a grid with nonuniform spacings ranging from 10 m to 40 m. The nonuniform grid is essential for modeling inhomogeneous conductivity structures. The grid consists of 215 nodes in x and 121 nodes in z, with its left and right boundaries located at $x = -2650$ m and $x = 3330$ m, respectively. The bottom boundary is at $z = 2575$ m. The numerical computation was initiated by assigning analytically computed field values at every node for $q = 0.12\sqrt{s}$ and $q = 0.12\sqrt{s} + \Delta q$, with the sampling interval of $\Delta q = 6 \times 10^{-4}\sqrt{s}$. It took 3 minutes on an IBM3090 computer (equivalent to 60 minutes on the VAX780) for 600 q steps; the result at $x = 1540$ m is shown in Figure 4 along with the analytic solution obtained from equation (A-15) of Appendix A. The agreement between these solutions is excellent.

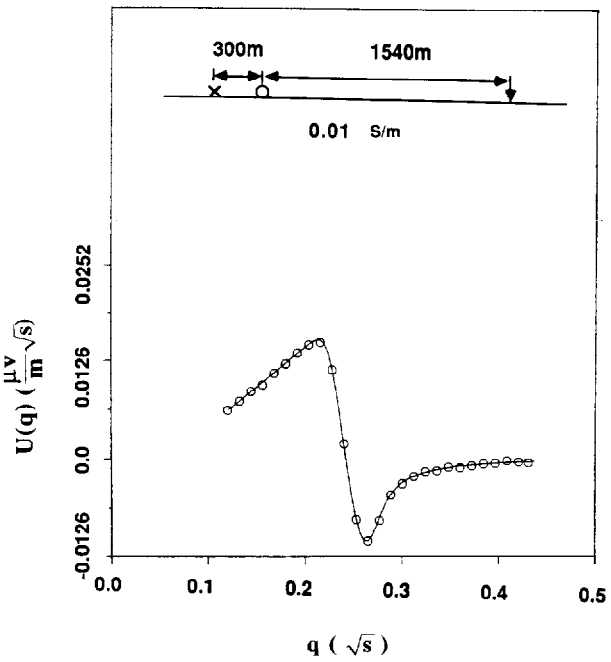

FIG. 4. Comparison of analytical (solid line) and numerical (circles) solutions for the wave field $\mathbf{U}(q)$ in the q domain on a half-space of 0.01 S/m. Two line current sources of opposite signs, separated by 300 m, are used with the positive one at the origin. The waveform of the current source is Gaussian. The position at which the wave field is displayed is at 1540 m.

The next model, shown in Figure 5, is a rectangular conductor of 1 S/m buried in a homogeneous earth of 0.01 S/m. The size of the conductor is 20 m in x and 300 m in z. The top of the conductor is 100 m below the surface of the earth and the left edge of the body is at $x = 300$ m. The source is the same as the one previously used except that the distance between the two line currents is now 500 m, with the positive current still located at the origin.

In this example, instead of solving for the total field as was done in the previous case, we have solved for the secondary field by reformulating equation (14) for the secondary field as

$$\nabla^2 U^s - \mu\sigma \frac{\partial^2}{\partial q^2} U^s = \mu\Delta\sigma \frac{\partial^2}{\partial q^2} U^i, \tag{18}$$

where superscripts i and s denote "incident" and "secondary," respectively; $\Delta\sigma$ is defined as the conductivity of the inhomogeneity minus that of the host medium. The direct time-domain equivalent of this approach has been adopted by Adhidjaja et al. (1985), resulting in improved accuracy in the numerical solution with decreased computer time. In particular, this formulation is useful when the scatterer is close to the source. Entering the source field in the immediate vicinity of the source is not necessary. The secondary field formulation requires "delayed" source terms in q, since the geometric separation between the source and the inhomogeneity guarantees that the secondary field is zero everywhere until after the source field arrives at the inhomogeneity.

The grid in this case consists of 129 nodes in x and 169

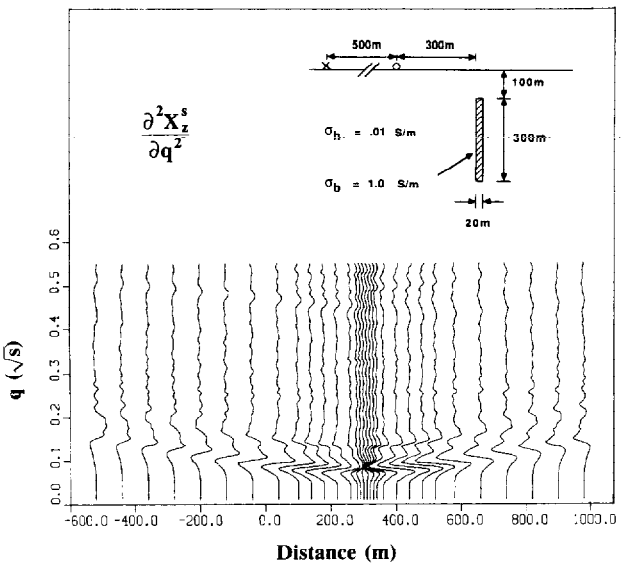

Fig. 5. Traces of the secondary wave fields $\partial^2 X_z^s/\partial q^2$ scattered by a 1 S/m conductor of size 20 m by 300 m. The conductor is buried in a half-space of 0.01 S/m, with its top 100 m below the surface. Two line sources separated by 500 m are used, with the positive current at the origin. The conductor is located at 300 m to the right of the origin. Wave-field amplitudes are relative.

nodes in z, with the left and right boundaries of the computational domain located at $x = -520$ m and $x = 1140$ m, respectively. The bottom boundary is at $z = 900$ m. The spacings, Δx and Δz, range from 2.5 m to 20 m, and the sampling in q is fixed at $\Delta q = 1.5 \times 10^{-4}\ \sqrt{\text{s}}$. Constants used to define the source function in this case are $q_0 = 0.03\sqrt{\text{s}}$ and $\alpha = 0.005\sqrt{\text{s}}$. Since the wave field has much slower speed inside the conductor, substantially smaller spacings should be used there. As a result, the step size in q is also reduced. The initial condition is set by assigning zero fields everywhere at $q = 0.01\sqrt{\text{s}} - \Delta q$ and $q = 0.01\sqrt{\text{s}}$. At these instants in q, the incident field has not arrived at the scatterer. The computer time required to carry out the 3600 q steps on the IBM3090 was 12 minutes.

The spatial derivatives of the secondary wave fields U^s computed in this manner are shown in Figures 5 and 6 in the form of

$$\frac{\partial^2 X_z^s}{\partial q^2} = -\frac{1}{\mu}\frac{\partial U^s}{\partial x},$$

corresponding to the time derivative of the vertical magnetic field, and

$$\frac{\partial^2 X_x^s}{\partial q^2} = \frac{1}{\mu}\frac{\partial U^s}{\partial z},$$

the time derivative of the horizontal magnetic field in the q domain. Here X is recognized as the transformed magnetic field in the q domain [$H(t) \rightarrow X(q)$]. The second-order derivative of $X(q)$ with respect to q is equivalent to the first-order derivative with respect to time. No additional computations are necessary, since the process of taking derivatives of the field with respect to x and z is a part of the finite-difference scheme. These figures show traces of wave fields in q at various positions on the surface. The amplitudes in both figures are relative. The conversion of the wave field to the time-domain EM field involves a simple integration given by equation (11). If we wish to obtain time-domain results corresponding to a specific source form, however, this integration should be modified accordingly. This is discussed in Appendix C, in which a particular case of reconstructing time-domain responses caused by a step-current source from wave fields generated by a Gaussian source is explained. The technique is general and can be easily adapted to simulating other forms of source. Using the modified integral equation (C-6) of Appendix C, we have transformed the responses for the station at $x = 200$ m of Figures 5 and 6 into the time domain. These are the time derivatives of the secondary magnetic fields. A comparison is made between these results and the corresponding direct

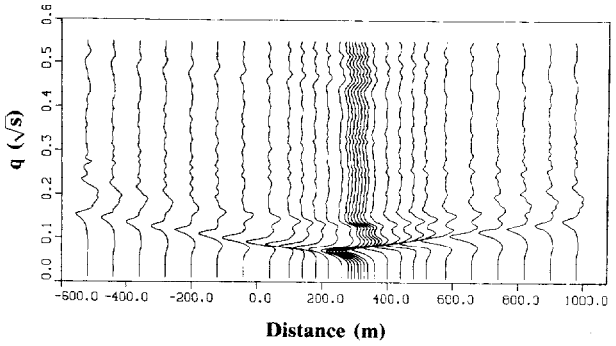

FIG. 6. Traces of the secondary wave fields $\partial^2 X_x^s/\partial q^2$ scattered by a 1 S/m conductor of size 20 m by 300 m in Figure 5. Once again, wave-field amplitudes are relative.

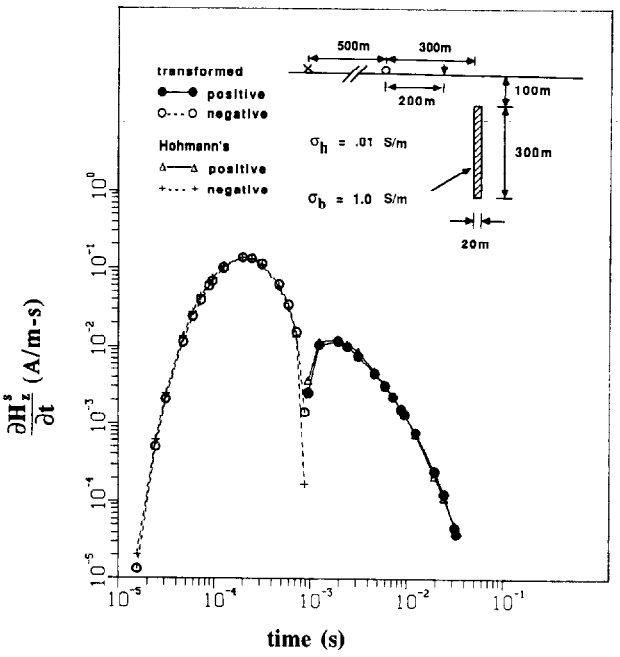

FIG. 7. Comparison between transformed and direct time-domain solutions for the time derivative of the secondary vertical magnetic field $\partial H_z^s/\partial t$ at the surface, $x = 200$ m.

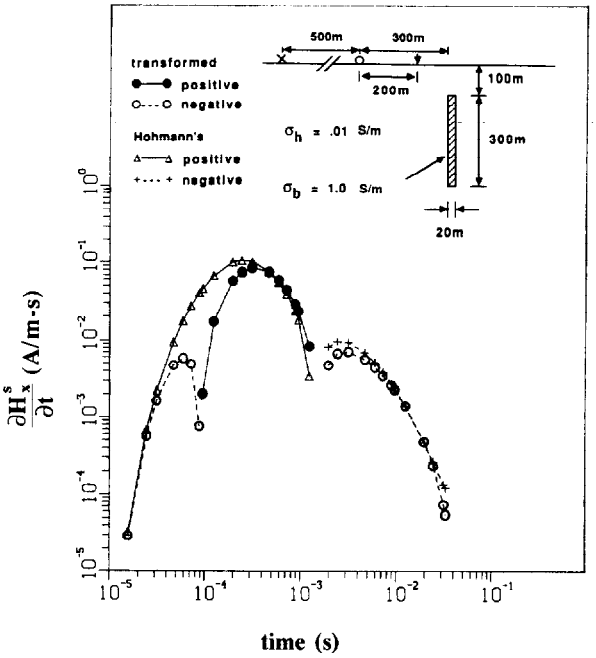

FIG. 8. Comparison between transformed and direct time-domain solutions for the time derivative of the secondary horizontal magnetic field $\partial H_x^s/\partial t$ at the surface, $x = 200$ m.

time-domain solutions provided by Hohmann (Pers. commun., 1988) in Figures 7 and 8. The two solutions are identical for the time derivative of the vertical magnetic field (Figure 7). The horizontal components of these solutions, however, show substantial difference in the early-time response (Figure 8). The solution obtained by the transform method experiences an early-time phase reversal.

Adding the analytically computed time-domain incident field to the numerically computed and transformed secondary field, we next show the profiles of the resulting emf, i.e., the voltage measured by a point coil with unit area. For time channels of t = 1, 5, 9, 15, 25, and 35 ms, the vertical component is displayed in Figure 9 and the horizontal component in Figure 10. The responses in the early-time channels for up to t = 25 ms agree very well with those from direct time-domain results presented by Oristaglio and Hohmann (1984). For the last channel, for t = 35 ms, however, the profiles of two solutions differ slightly across the top of the conductor. The solution obtained from the q-domain approach is not as smooth as the direct time-domain solution, indicating that more q-step numerical solutions may be required for better results.

A FORMULATION FOR 3-D PROBLEMS

In this section we introduce a new approach for modeling 3-D EM problems in the transformed domain. As a result, numerical techniques developed for solving wave equations can be applied directly to the formulation presented here. In source-free regions, Maxwell's equations in the transformed domain become

$$\nabla \times \mathbf{U} = -\mu \frac{\partial^2}{\partial q^2} \mathbf{X} \tag{19}$$

and

$$\nabla \times \mathbf{X} = \sigma \mathbf{U}. \tag{20}$$

In these equations the displacement current has been neglected, and all independent variables have been omitted for simplicity. We also notice that $\mathbf{E}(t)$ and $\mathbf{H}(t)$ have been transformed to $\mathbf{U}(q)$ and $\mathbf{X}(q)$, respectively. Introducing a change of variable

$$\mathbf{V} = \frac{\partial}{\partial q} \mathbf{X},$$

equation (19) becomes

$$\nabla \times \mathbf{U} = -\mu \frac{\partial}{\partial q} \mathbf{V}; \tag{21}$$

taking the derivative of equation (20) with respect to q, we find that

$$\nabla \times \mathbf{V} = \sigma \frac{\partial}{\partial q} \mathbf{U}. \tag{22}$$

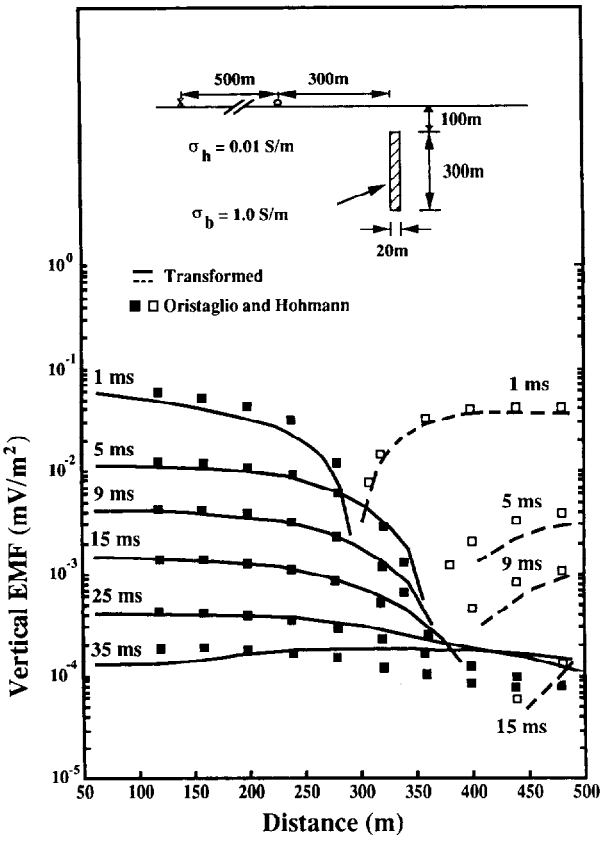

FIG. 9. Comparison between transformed and direct time-domain solutions for the vertical emf at 1, 5, 9, 15, 25, and 35 ms. Solid lines and dark squares are positive, and broken lines and open squares are negative.

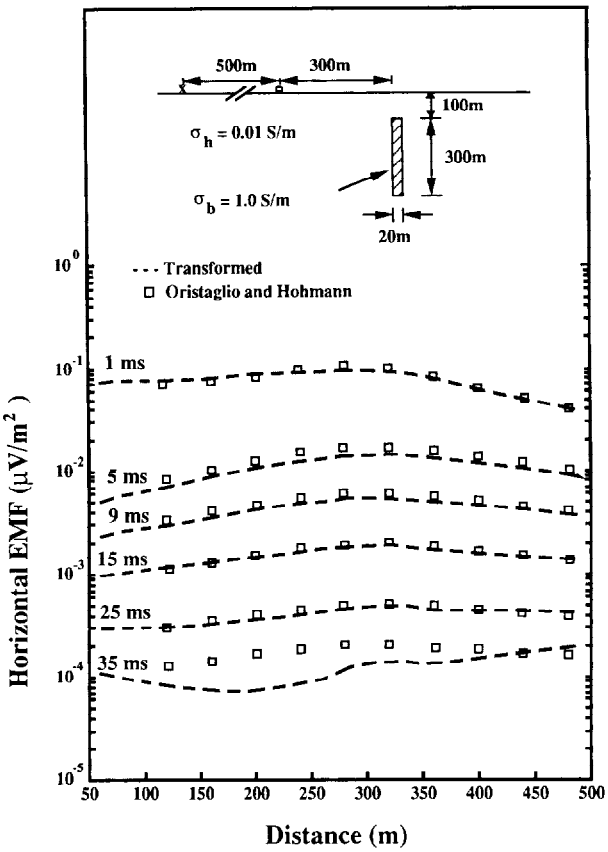

FIG. 10. Comparison between transformed and direct time-domain solutions for the horizontal emf at 1, 5, 9, 15, 25, and 35 ms. All values are negative.

Equations (21) and (22) are a system of wave equations for **U** and **V** and can be formally rewritten as

$$\left(\underline{\mathbf{A}}\frac{\partial}{\partial x}+\underline{\mathbf{B}}\frac{\partial}{\partial y}+\underline{\mathbf{C}}\frac{\partial}{\partial z}+\underline{\mathbf{D}}\frac{\partial}{\partial q}\right)\mathbf{W}=\mathbf{0}, \tag{23}$$

where $\underline{\mathbf{A}}$, $\underline{\mathbf{B}}$, $\underline{\mathbf{C}}$, and $\underline{\mathbf{D}}$ are symmetric matrices of order 6 with zero entries except

$$a_{26}=a_{62}=b_{34}=b_{43}=c_{15}=c_{51}=1,$$

$$a_{35}=a_{53}=b_{16}=b_{61}=c_{24}=c_{42}=-1,$$

and

$$d_{ii}=\sigma \quad \text{for} \quad i=1,2,3 \quad \text{and} \quad =\mu \quad \text{for} \quad i=4,5,6.$$

W is a column vector consisting of Cartesian components of vector wave fields **U** and **V**

$$\mathbf{W}=(U_x, U_y, U_z, V_x, V_y, V_z)^T.$$

Note that elements of matrices $\underline{\mathbf{A}}$, $\underline{\mathbf{B}}$, and $\underline{\mathbf{C}}$ are constant and independent of spatial variables and also that the matrix $\underline{\mathbf{D}}$ is independent of the variable q. This property enables us to rewrite equation (23) in a more compact form

$$\boldsymbol{\Omega}\cdot\mathbf{Y}=0,$$

where the vector function **Y** is given by

$$\mathbf{Y}=(\hat{\mathbf{x}}^T\underline{\mathbf{A}}\mathbf{W})\hat{\mathbf{x}}+(\hat{\mathbf{y}}^T\underline{\mathbf{B}}\mathbf{w})\hat{\mathbf{y}}+(\hat{\mathbf{z}}^T\underline{\mathbf{C}}\mathbf{w})\hat{\mathbf{z}}+(\hat{\mathbf{q}}^T\underline{\mathbf{D}}\mathbf{w})\hat{\mathbf{q}}$$

and the operator $\boldsymbol{\Omega}$ is defined as

$$\boldsymbol{\Omega}=\frac{\partial}{\partial x}\hat{\mathbf{x}}+\frac{\partial}{\partial y}\hat{\mathbf{y}}+\frac{\partial}{\partial z}\hat{\mathbf{z}}+\frac{\partial}{\partial q}\hat{\mathbf{q}}.$$

Equations of the form of equation (23) are called divergence-free. An excellent analysis for the stability and the accuracy of the resulting numerical solution to this type of equation has been given by Strang (1968). It is to this particular form of equation that the dimensional splitting method (Strang, 1968), among other techniques, can be applied efficiently. In this method, a multidimensional problem is simulated by a sequence of 1-D problems; consequently the complexity involved in the numerical treatment of boundary values is substantially reduced. The algorithm based on the dimensional splitting method has been applied successfully to elastic waves in 2-D media by Bayliss et al. (1986).

CONCLUSIONS

The successful application of the transform method to the numerical modeling of EM fields has been demonstrated. The approach provides a powerful new method with which we can compute numerical solutions for many practical geologic models. The physical meaning of the wave field in the q domain is not entirely clear at the moment. The approach simply makes use of advantages inherent in methods of solving the wave equation for the diffusion equations.

For direct time-domain solutions the time step Δt for the explicit numerical method is determined by the grid diffusion time (Potter, 1973). For typical earth materials the range of grid diffusion time is less than 1 μs. It has been shown, however, that this rather severe constraint in the time-step size can be gradually relaxed as time increases (Oristaglio and Hohmann, 1984). This finding is based on the slowing down of the diffusion rate of the point-source field in an unbounded medium. Numerical modeling involves complicated interactions among inhomogeneities, and each one of these inhomogeneities acts as a source at all time. For this reason, the increased time-stepping scheme should be used as a guide, and care should be taken when the scheme is applied to modeling of EM fields for general conductivity structures. In the transform domain, on the other hand, the increment in q is dictated strictly by the CFL stability condition [see equation (15)]. This condition results in a range of Δq from approximately 0.1 mq to 1 mq for the same typical earth materials. For example, let us assume a model consisting of a 2-D medium with its conductivity distribution ranging from 0.01 S/m to 1.0 S/m. In this case, the ratio of the minimum velocity to the maximum velocity is 0.1. The constant α used to define the Gaussian waveform is $0.01\sqrt{s}$. Substituting these numbers into equation (17), we find that the maximum Δq is 0.44 mq. Based on this consideration, we initially thought that the q-domain approach would be much faster computationally than the time-domain approach. However, present model study shows that actual q-domain computing time is about the same as those reported by Oristaglio and Hohmann (1984) and Adhidjaja et al. (1985). Nonetheless, as an initial demonstration we consider this near equality in computing time to be a major accomplishment, since the technique is new and significant reduction in computing time could result if the scheme can be optimized.

In principle, the optimization can be achieved by using higher order absorbing boundary conditions (Clayton and Enquist, 1977). Successfully implemented, the domain of computation would be reduced; as a result, overall computer time would be decreased. Another major gain in speed could be achieved by using the finite-element method instead of the finite-difference method. The relative freedom in choosing the shape of elements in the finite-element method would considerably reduce the total number of cells within the numerical boundaries. Because of the requirement of having to use straight lines to discretize a model, the finite-difference scheme involves needless rectangular elements on all four sides of the conductive body. The number of unnecessary elements would increase as we increased the conductivity contrast. The finite-element scheme can reduce this waste but at the expense of increased complexity in grid designing to avoid spurious reflections in the numerical solution.

Our ultimate goal is the development of 3-D numerical modeling techniques that can be used to interpret practical EM sounding data. Although the proposed technique appears promising, practical use of the resulting computer program for routine interpretations would still require modern computer capabilities.

ACKNOWLEDGMENT

This work was supported by the Director, Office of Energy Research, Office of Basic Energy Sciences, Engineering and Geosciences Division, of the U.S. Department of Energy under contract no. DE-AC03-76SF00098.

REFERENCES

Adhidjaja, J. I., Hohmann, G. W., and Oristaglio, M. L., 1985, Two-dimensional transient electromagnetic responses: Geophysics, **50**, 2849–2861.

Bayliss, A., Jordan, K. E. LeMesurier, B. J., and Turkel, E., 1986, A fourth-order accurate finite-difference scheme for the computation of elastic waves: Bull. Seis. Soc. Am., **76**, 1115–1132.

Best, M. E., Duncan, P., Jacobs, F. J., and Scheen, W. L., 1985, Numerical modeling of the electromagnetic response of three-dimensional conductors in a layered earth: Geophysics, **50**, 665–676.

Clayton, R., and Enquist, B., 1977, Absorbing boundary conditions for acoustic and elastic wave equations: Bull. Seis. Soc. Am., **67**, 1529–1541.

Filatov, V. V., 1984, Construction of focusing transformations of transient electromagnetic fields: Geol. i Geofiz. (Soviet Geology and Geophysics), **25**, 89–95.

Goldman, Y., Hubans, C., Nicoletis, S., and Spitz, S., 1986, A finite-element solution for the transient electromagnetic response of an arbitrary two-dimensional resistivity distribution: Geophysics, **51**, 1450–1461.

Gupta, P. K., Bennett, L. A., and Raiche, A. P., 1987, Hybrid calculations of the three-dimensional electromagnetic response of buried conductors: Geophysics, **52**, 301–306.

Harrington, R. F., 1961, Time-harmonic electromagnetic fields: McGraw-Hill Book Co.

Hohmann, G. W., 1975, Three-dimensional induced polarization and electromagnetic modeling: Geophysics, **40**, 309–324.

Isaev, G. A., and Filatov, V. V., 1981, Physicomathematical principles of visualization of nonstationary electromagnetic fields: Geol. i Geofiz. (Soviet Geology and Geophysics), **22**, 89–95.

Kunetz, G., 1972, Processing and interpretation of magnetotelluric soundings: Geophysics, **37**, 1005–1021.

Kuo, J. T., and Cho, D. H., 1980, Transient time-domain electromagnetics: Geophysics, **45**, 271–291.

Lavrent'ev, M. M., Romanov, V. G., and Shishatskii, S. P., 1980, Ill-posed problems of mathematical physics and analysis (in Russian): Nauka.

Lee, K. H., 1987, A new approach to modeling and interpreting electromagnetic sounding data: Lawrence Berkeley Laboratory, Rep. LBL-23544.

Lee, K. H., Pridmore, D. F., and Morrison, H. F., 1981, A hybrid three-dimensional electromagnetic modeling scheme: Geophysics, **46**, 796–805.

Levy, S., Oldenburg, D., and Wang, J., 1988, Subsurface imaging using magnetotelluric data: Geophysics, **53**, 104–117.

Lines, L. R., and Jones, F. W., 1975, The perturbation of alternating geomagnetic fields by three-dimensional island structures: Geophys. J. Roy. Astr. Soc., **32**, 133–154.

Meyer, W. H., 1977, Computer modeling of electromagnetic prospecting methods: Ph.D. thesis, Univ. Calif., Berkeley.

Mitchel, A. R., and Griffiths, D. F., 1980, The finite difference method is partial differential equations: John Wiley and Sons.

Newman, G. A., and Hohmann, G. W., 1988, Transient electromagnetic responses of high-contrast prisms in a layered earth: Geophysics, **53**, 691–706.

Oristaglio, M. L., and Hohmann, G. W., 1984, Diffusion of electromagnetic fields into a two-dimensional earth: A finite-difference approach: Geophysics, **49**, 870–894.

Potter, D., 1973, Computational physics: John Wiley and Sons.

Pridmore, D. F., 1978, Three-dimensional modeling of electric and electromagnetic data using the finite-element method: Ph.D. thesis, Univ. of Utah.

Raiche, A. P., 1974, An integral equation approach to 3D modeling: Geophys. J. Roy. Astr. Soc., **36**, 363–376.

Reddy, I. K., Rankin, D., and Phillips, R. J., 1977, Three-dimensional modeling in magnetotelluric and magnetic variational sounding: Geophys. J. Roy. Astr. Soc., **51**, 313–326.

San Filipo, W. A., and Hohmann, G. W., 1985, Integral equation solution for the transient electromagnetic response of a three-dimensional body in a conductive half-space: Geophysics, **50**, 798–809.

Scheen, W. L., 1978, EMMMMA, a computer program for three-dimensional modeling of airborne electromagnetic surveys: Proc. Workshop on Modeling of Electric and Electromagnetic Methods, Lawrence Berkeley Laboratory, LBL-7053, 53.

Strang, G., 1968, On the construction and comparison of difference schemes: SIAM J. Numer. Anal., **5**, 506–517.

Weidelt, P., 1972, The inverse problem of geomagnetic induction: Zeit. fur Geophys., **38**, 257–298.

——— 1975, Electromagnetic induction in three-dimensional structures: J. Geophysics., **41**, 85–109.

APPENDIX A

PRIMARY ELECTRIC FIELD IN THE TRANSFORMED DOMAIN

Here we derive the Green's function for the electric field in the q domain due to a line current source on the surface of a homogeneous earth. A right-hand coordinate is chosen such that the $x - y$ plane coincides with the earth surface and the z-axis points vertically down. Let the source line merge with the y-axis and the current flow in the positive y direction. Once the Green's function corresponding to an impulsive source is found, the function is convolved with a source function $F(q)$ to yield the primary field. This primary field is used in the finite-difference computation.

The 2-D electric Green's function $G(x, y, q)$ with the displacement current neglected satisfies the following equations:

$$\nabla^2 G(x, z, q) = 0, \qquad z < 0 \tag{A-1}$$

and

$$\left(\nabla^2 - \mu\sigma \frac{\partial^2}{\partial q^2}\right) G(x, z, q) = 0, \qquad z > 0, \tag{A-2}$$

where μ is the magnetic permeability and σ the conductivity of the earth. Taking the Fourier transform of the above equations with respect to x and q, we get

$$\left(-k_x^2 + \frac{\partial^2}{\partial z^2}\right) \tilde{G}(k_x, z, \nu) = 0, \qquad z < 0 \tag{A-3}$$

and

$$\left(-k_x^2 + \mu\sigma\,\nu^2 + \frac{\partial^2}{\partial z^2}\right) \tilde{G}(k_x, z, \nu) = 0, \qquad z > 0, \tag{A-4}$$

where

$$\tilde{G}(k_x, z, \nu) = \int\int_{-\infty}^{+\infty} G(x, z, q) e^{-i(k_x x + \nu q)}\, dx\, dq.$$

Solutions to equations (A-3) and (A-4) in their respective regions are

$$\tilde{G}(k_x, z, \nu) = A(k_x, \nu) e^{|k_x| z}, \qquad z < 0 \tag{A-5}$$

and

$$\tilde{G}(k_x, z, \nu) = B(k_x, \nu) e^{-ik_z z}, \qquad z > 0, \tag{A-6}$$

with

$$k_z = -i\sqrt{k_x^2 - \mu\sigma\nu^2}, \qquad k_x^2 > \mu\sigma\,\nu^2$$

and

$$k_z = \sqrt{\mu\sigma\nu^2 - k_x^2}, \qquad k_x^2 < \mu\sigma\,\nu^2.$$

We now apply boundary conditions to these solutions at $z = 0$. From the continuity of the tangential electric field

$$A = B, \tag{A-7}$$

and from the discontinuity of the tangential magnetic field across the surface current (Harrington, 1961)

$$-|k_x|A - ik_zB = -1, \tag{A-8}$$

we obtain

$$A = B = \frac{1}{|k_x| + ik_z} = \frac{1}{\mu\sigma}\frac{|k_x| - ik_z}{\nu^2}. \tag{A-9}$$

The Green's function on or below the surface of the earth ($z > 0$) can now be formally written as

$$G(x, z, q) = \frac{1}{4\pi^2\mu\sigma} \times \int\int_{-\infty}^{+\infty} \frac{|k_x| - ik_z}{\nu^2} e^{-ik_z z} e^{i(k_x x + \nu q)}\, dk_x\, d\nu. \tag{A-10}$$

The inverse Fourier transform in equation (A-10) can be carried out by writing

$$G(x, z, q) = I_1 + I_2,$$

with

$$I_1 = \frac{1}{4\pi^2\mu\sigma}\int\int_{-\infty}^{+\infty}\frac{|k_x|}{\nu^2} e^{-ik_z z} e^{i(k_x x + \nu q)}\, dk_x\, d\nu$$

and

$$I_2 = -\frac{1}{4\pi^2\mu\sigma}\int_{-\infty}^{+\infty}\frac{ik_z}{\nu^2} e^{-ik_z z} e^{i(k_x x + \nu q)}\, dk_x\, d\nu,$$

and evaluating integrals term by term. The first term, I_1, can be evaluated by initially making a change of variables $s = i\nu$ and subsequently manipulating the expression into

$$I_1 = \frac{1}{\pi\mu\sigma}\frac{\partial^2}{\partial x\,\partial z} \times \int_0^{+\infty}\left[\frac{1}{2\pi i}\int_{-i\infty}^{+i\infty}\frac{e^{-\sqrt{k_x^2 + \mu\sigma s^2}\,z}}{s^2\sqrt{k_x^2 + \mu\sigma s^2}} e^{sq}\, ds\right]\sin k_x x\, dk_x.$$

In this integral, all possible k_z values that satisfy radiation conditions have been accounted for. The inverse Laplace transform in the brackets can be written as a convolution of a linearly increasing function

$$L^{-1}\left(\frac{1}{s^2}\right) = q, \qquad q > 0,$$

with a Bessel function of the first kind of zero order:

$$L^{-1}\left(\frac{e^{-\sqrt{k_x^2 + \mu\sigma s^2}\,z}}{\sqrt{k_x^2 + \mu\sigma s^2}}\right) = \begin{cases} 0, & 0 < q < \sqrt{\mu\sigma}\,z \\ \dfrac{1}{\sqrt{\mu\sigma}} J_0\left(\dfrac{k_x}{\sqrt{\mu\sigma}}\sqrt{q^2 - \mu\sigma z^2}\right), & q > \sqrt{\mu\sigma}\,z. \end{cases}$$

Thus, with $\rho^2 = x^2 + z^2$, we obtain

$$I_1 = 0, \qquad 0 < q < \sqrt{\mu\sigma z}$$

and

$$I_1 = \frac{1}{\pi\mu\sigma}\frac{\partial^2}{\partial x\,\partial z}\left[q * \int_0^{+\infty}\frac{1}{\sqrt{\mu\sigma}} \times J_0\left(\frac{k_x}{\sqrt{\mu\sigma}}\sqrt{q^2 - \mu\sigma z^2}\right)\sin k_x x\, dk_x\right]$$

$$= \begin{cases} \dfrac{1}{\pi\mu\sigma}\dfrac{\partial^2}{\partial x\,\partial z}\displaystyle\int_{\sqrt{\mu\sigma z}}^{q}\frac{q - \tau}{\sqrt{\mu\sigma\rho^2 - \tau^2}}\, d\tau, \\ \qquad\qquad \sqrt{\mu\sigma z} < q < \sqrt{\mu\sigma\rho} \\ \dfrac{1}{\pi\mu\sigma}\dfrac{\partial^2}{\partial x\,\partial z}\displaystyle\int_{\sqrt{\mu\sigma z}}^{\sqrt{\mu\sigma\rho}}\frac{q - \tau}{\sqrt{\mu\sigma\rho^2 - \tau^2}}\, d\tau, \\ \qquad\qquad q > \sqrt{\mu\sigma\rho}, \end{cases} \tag{A-11}$$

where the $*$ denotes convolution. The second term, I_2, can be evaluated by rewriting I_2 as

$$I_2 = \frac{i}{4\pi\mu\sigma}\frac{\partial^2}{\partial z^2}\int_{-\infty}^{+\infty}\frac{e^{i\nu q}}{\nu^2}\left(\frac{1}{\pi}\int_{-\infty}^{+\infty}\frac{e^{-ik_z z}}{k_z}\cos k_x x\, dk_x\right)d\nu$$

$$= \frac{i}{4\pi\mu\sigma}\frac{\partial^2}{\partial z^2}\int_{-\infty}^{+\infty}\frac{H_0^{(2)}(\sqrt{\mu\sigma\rho\nu})}{\nu^2} e^{i\nu q} d\nu$$

$$= \begin{cases} 0, & q < \sqrt{\mu\sigma\rho} \\ \dfrac{1}{\pi\mu\sigma}\dfrac{\partial^2}{\partial z^2}\displaystyle\int_{\sqrt{\mu\sigma\rho}}^{q}\frac{q - \tau}{\sqrt{\tau^2 - \mu\sigma\rho^2}}\, d\tau, & q > \sqrt{\mu\sigma\rho}. \end{cases} \tag{A-12}$$

The integrations and differentiations involved in equations (A-11) and (A-12) can be carried out in closed forms to yield

$$G(x, z, q) = 0, \qquad 0 < q < \sqrt{\mu\sigma z},$$

$$= \frac{1}{\pi\mu\sigma\rho^4}\left[(x^2 - z^2)q + \frac{|x|z(2q^2 - \mu\sigma\rho^2)}{\sqrt{\mu\sigma\rho^2 - q^2}}\right], \qquad \sqrt{\mu\sigma}\,z < q < \sqrt{\mu\sigma\rho},$$

$$= \frac{1}{\pi\mu\sigma\rho^4}\left[(x^2 - z^2)q - x^2\sqrt{q^2 - \mu\sigma\rho^2} + \frac{z^2q^2}{\sqrt{q^2 - \mu\sigma\rho^2}}\right], \qquad q > \sqrt{\mu\sigma\rho}. \tag{A-13}$$

On the surface of the earth ($z = 0$), this Green's function reduces to

$$G(x, z = 0, q) = \begin{cases} \dfrac{q}{\pi\mu\sigma\, x^2}, & 0 < q < \sqrt{\mu\sigma}x \\ \dfrac{1}{\pi\mu\sigma x^2}(q - \sqrt{q^2 - \mu\sigma x^2}), & q > \sqrt{\mu\sigma}x. \end{cases} \quad \text{(A-14)}$$

Now that the Green's function has been found, the incident electric field U^i in the transformed domain due to a corresponding source function $F(q)$ can be computed by a convolution:

$$U^i(x, z, q) = \int_0^{+\infty} G(x, z, q - \tau)F(\tau)\, d\tau. \quad \text{(A-15)}$$

In our computation, we have chosen $F(q)$ to be a Gaussian bell given by

$$F(q) = e^{-(q - q_0)^2/2\alpha^2}. \quad \text{(A-16)}$$

In equation (A-16), constant parameter q_0 and α effectively control the waveform. Typical values used in this study are $q_0 = 0.03\sqrt{s}$ and $\alpha = 0.005\sqrt{s}$.

APPENDIX B

BOUNDARY CONDITIONS

The finite-difference method involves discretization of a domain confined by a closed boundary, where special treatments are required for its boundary values. In order to make the computational domain as small as possible, it has been shown that absorbing boundary conditions can be used for modeling wave-field propagation (Clayton and Enquist, 1977). Since q-domain modeling is essentially a wave propagation problem, we applied the absorbing boundary conditions (a second order in Clayton and Enquist, 1977) to the side and bottom boundaries of our 2-D models.

The upper boundary is the air-earth interface. The air is excluded from the computational domain. In this section we discuss how we treat this boundary value problem numerically. An excellent scheme for the treatment of time-domain boundary conditions at the air-earth interface has been given by Oristaglio and Hohmann (1984). The q-domain equivalent takes the same form and can be written as

$$\frac{\partial}{\partial z} U(x, z = 0, q) = \frac{1}{\pi} P \int_{-\infty}^{+\infty} dx' \frac{\partial_x U(x', z = 0, q)}{x - x'}, \quad \text{(B-1)}$$

where P indicates the Cauchy principal value. This equation relates the vertical derivative of the electric field to the Hilbert transform of its horizontal derivative. We now consider a fictitious boundary Δz above the earth's surface. The size of the extension Δz is the same as the vertical sampling interval just below the earth's surface. If the electric field at $q = i\Delta q$ at this extended boundary is known, the electric field at $q = (i + 1)\Delta q$ inside the boundary, specifically at the air-earth interface, can be computed by rearranging the numerical expression for

$$\left(\frac{\partial^2}{\partial x^2} + \frac{\partial^2}{\partial z^2} - \mu\sigma \frac{\partial^2}{\partial q^2}\right) U(x, z = 0, q) = 0. \quad \text{(B-2)}$$

Using the vertical derivative of the electric field obtained from equation (B-1), we compute the electric field at the fictitious level $z = -\Delta z$ from the central-difference scheme

$$U(x, z = -\Delta z, q) = U(x, z = \Delta z, q) - 2\Delta z \frac{\partial U(x, z = 0, q)}{\partial z}, \quad \text{(B-3)}$$

and then substitute this result at $z = -\Delta z$ into equation (B-2) to finally obtain the electric field at the next q step at the air-earth interface.

At the air-earth interface, numerical computations for the Hilbert transform are carried out in the wavenumber domain, using the Fourier transform equivalent of equation (B-1)

$$\frac{\partial U(k_x, z = 0, q)}{\partial z} = |k_x| U(k_x, z = 0, q). \quad \text{(B-4)}$$

A Lagrange interpolation scheme is used to interpolate field values generated by the finite-difference on the nonuniform grid to field values on a uniform grid. These interpolated field values are then Fourier transformed and used as in equation (B-4) for the wavenumber-domain Hilbert transform.

APPENDIX C

TRANSFORMATION OF FIELDS

In the q-domain numerical modeling, the source function needs to be both finite and sufficiently smooth so that serious dispersions effected by the discretization in both space and q can be avoided. For this reason, we have chosen a Gaussian pulse as the source throughout this paper. The objective here is then to recover the anticipated time-domain step-current response from the q-domain numerical model result with a Gaussian type of source.

The relation between q-domain and time-domain fields is given by

$$E(t) = \frac{1}{2\sqrt{\pi t^3}} \int_0^{\infty} q e^{-q^2/4t} U(q)\, dq. \quad \text{(C-1)}$$

Taking the Fourier transform of equation (C-1) with respect to t, we find

$$\tilde{E}(\omega) = \int_0^\infty e^{-\sqrt{i\omega}q} U(q)\, dq. \tag{C-2}$$

Rewriting the Gaussian source function given by equation (A-16) in Appendix A,

$$F(q) = e^{-(q-q_0)^2/2\alpha^2},$$

and choosing constant parameters q_0 and α such that $F(q)$ remains effectively zero for q less than zero, we can show that the Fourier transform of the time-domain equivalent of this source is

$$\tilde{S}(\omega) = \sqrt{2\pi}\alpha e^{-\sqrt{i\omega}\, q_0 + i\omega\alpha^2/2}. \tag{C-3}$$

The frequency spectrum of the time-domain response due to the unit step-current source, therefore, can be written as a deconvolution

$$\tilde{I}(\omega) = \mu \frac{\tilde{E}(\omega)}{\tilde{S}(\omega)}$$

$$= \frac{\mu}{\sqrt{2\pi}\alpha} \int_0^\infty e^{-\sqrt{i\omega}(q-q_0) - i\omega\alpha^2/2} U(q)\, dq. \tag{C-4}$$

We now require that the secondary wave field scattered by the conductor not reach the earth's surface before $q = q_0$, so that

$$U(q) = 0, \qquad q < q_0. \tag{C-5}$$

Then the response due to the step-current source can be obtained by taking the inverse Fourier transform of equation (C-4); the result is

$$I(t) = 0, \qquad t < \frac{\alpha^2}{2},$$

$$= \frac{\mu}{2\pi\alpha\sqrt{2(t-\alpha^2/2)^3}}$$

$$\times \int_{q_0}^\infty (q-q_0) e^{-\frac{(q-q_0)^2}{4(t-\alpha^2/2)}} U(q)\, dq, \qquad t > \frac{\alpha^2}{2}. \tag{C-6}$$